Vol. 283: 39–54, 2004 | MARINE ECOLOGY PROGRESS SERIES
Mar Ecol Prog Ser | Published November 30

Cycling of dissolved and particulate carbohydrates in a coastal upwelling system (NW Iberian Peninsula)

M. Nieto-Cid*, X. A. Álvarez-Salgado, S. Brea, F. F. Pérez

CSIC, Instituto de Investigacións Mariñas, Eduardo Cabello 6, 36208 Vigo, Spain

ABSTRACT: The contribution of carbohydrates to the dissolved (DOC) and suspended (POC) organic carbon pools in NW Iberian shelf waters was assessed from May 2001 to April 2002. Particulate carbohydrates (p-CHO) represented 26 ± 1 and 12 ± 1% of the POC changes in the middle of the Ría de Vigo (50 m water) and the middle of the adjacent continental shelf (150 m water), respectively. The contribution of dissolved carbohydrates (d-CHO) to the DOC changes was larger than p-CHO: 29 ± 4% in the ría and 31 ± 4% in the shelf. The correlations between p-CHO and POC ($r = +0.88$, $n = 298$, $p < 0.001$) and between d-CHO and DOC ($r = +0.82$, $n = 298$, $p < 0.001$) indicate that carbohydrate changes are linked to bulk organic carbon changes within the time scale of the sampling frequency (2 wk). Maximum carbohydrate accumulation occurred during the upwelling season at the 'spin down' phase of upwelling events; estimated rates of d-CHO production in the middle of the ría were ~1.5 µmol C l^{-1} d^{-1}, an order of magnitude larger than during the winter period. Although monosaccharides represented 30 to 40% of the bulk d-CHO, they were responsible for less than 20% of the d-CHO changes, indicating that most of the freshly produced d-CHO is semi-labile sugar polymers.

KEY WORDS: Dissolved carbohydrates · Particulate carbohydrates · DOC · POC · Seasonal cycle · Coastal upwelling · NW Iberian Peninsula

Resale or republication not permitted without written consent of the publisher

INTRODUCTION

Although marine dissolved organic matter (DOM) is one of the largest active reservoirs of organic carbon in the biosphere (Hedges 1992, 2002) and is important for understanding the global carbon cycle and the changes in the concentration of atmospheric carbon dioxide (Siegenthaler & Sarmiento 1993), only a small portion of this pool has been identified. The major advances have been achieved with the combination of ultrafiltration methods (Amon & Benner 1996) and nuclear magnetic resonance techniques (Benner et al. 1992, Aluwihare et al. 1997, McCarthy et al. 1997, Clark et al. 1998, Hedges et al. 2002). Carbohydrates are one of the major products of marine phytoplankton photosynthesis and represent the main part of the known fraction of organic carbon in the water column (Benner 2002, Ogawa & Tanoue 2003). According to Pakulski & Benner (1994), dissolved carbohydrate accounts for 13 to 46% of the dissolved organic carbon (DOC) pool in seasonal thermocline waters, with significant differences between environments: the percentage is higher in the Pacific Ocean (~30%) and the Gulf of Mexico (~23%) than in the North Atlantic (~16%). In contrast, carbohydrates have been shown to represent from 50 (surface waters) to 25% (deep waters) of ultrafiltered DOM (UDOM) by ^{13}C nuclear magnetic resonance (NMR) (Benner et al. 1992), and 80 ± 4% by ^{1}H NMR (Aluwihare et al. 1997).

Particulate organic matter (POM) is a mixture of plankton and detritus with different elemental (C, H, O, N, P) and biochemical (proteins, carbohydrates, lipids, phosphorus compounds, pigments) compositions; detritus is richer in lipids and phytoplankton in proteins and carbohydrates (Ríos et al. 1998). The variability of particulate organic carbon (POC) is affected by the quality (ratio between plankton and detritus, predominance of diatoms or other autotrophs, het-

*Email: mmar@iim.csic.es

© Inter-Research 2004 · www.int-res.com

erotrophs, etc.) and the composition of the different groups. The Redfield formula ($C_{106}H_{171}O_{42}N_{16}P$) represents the average composition of the organic tissues of marine phytoplankton (Anderson 1995, Fraga 2001), which includes 23.4% (w/w) carbohydrates, although this ranges from 15 to 26% for plankton net tow samples from different marine environments (Hedges et al. 2002).

Several methods were used to determine dissolved carbohydrates until the 3-methyl-2-benzothiazolinone hydrazone (MBTH) colourimetric method was proposed by Burney & Sieburth (1977). This procedure is tedious and involves many steps. More recently, the colourimetric reagent 2,4,6-tripyridyl-*s*-triazine (TPTZ) has been suggested (Myklestad et al. 1997). These 2 methods agree well, especially in filtered seawater samples (Witter & Luther III 2002). They provide concentrations much higher than those obtained by molecular separation methods such as HPLC with pulsed amperometric detection (HPLC-PAD). The reasons for this divergence among methods are not yet very clear. The numerous difficulties in carbohydrate analysis, such as the low concentrations of free monosaccharides (Pakulski & Benner 1994), their high water solubility, the lack of a light-absorbing chromophore and the presence of multiple charge states at seawater pH (neutral sugars, positively charged amino sugars and negatively charged uronic acid), are behind the multiplicity of methods and the discrepancies between them.

A limited number of studies concerning the dissolved carbohydrate pool have been published over the last decade. Most of them refer to single transects sampled once (Bhosle et al. 1998, Hung et al. 2001, Witter & Luther III 2002) or twice (Pettine et al. 1999, Hung et al. 2003) in different environments. Only 1 annual cycle has been presented to date, by Børsheim et al. (1999), who sampled 2 inshore stations in the Trondheimsfjord (Norway) every month over 2 years. None of the above studies were devoted to oceanic or coastal upwelling areas.

Although ocean margins cover only 8% of the total ocean surface, according to different estimates they support 18 to 33% of the global net primary production and 27 to 50% of the global export production (Walsh 1991, Chavez & Toggweiler 1995, Wollast 1998). Coastal upwelling areas are particularly productive because of the enhanced entry of nutrients from the adjacent ocean. Therefore, they are probable sites of intensified carbohydrate production.

The western coast of the Iberian Peninsula is affected by intermittent periods of upwelling (1 to 2 wk, Álvarez-Salgado et al. 1999), with a marked seasonal cycle (Wooster et al. 1976). From April to October (the upwelling season), northerly winds cause Eastern North Atlantic Central Water (ENACW) to upwell over the shelf, penetrating from the bottom of the ría and enhancing the positive residual circulation pattern (Rosón et al. 1997). Transition from northerly to southerly winds occurs during the autumn (October to November). From November to March (the downwelling season), southerly winds prevail and a downwelling front develops at the slope, precluding shelf edge exchange (Castro et al. 1997). During the winter, a strong poleward flow of subtropical ENACW occurs along the slope (Haynes & Barton 1990, Álvarez-Salgado et al. 2003).

Studies of the role played by DOM in coastal upwelling systems are relatively scarce, and most of them have been conducted on the western coast of the Iberian Peninsula. These studies have confirmed that the Rías Baixas (which the Ria de Vigo is part of) are pre-eminent sites for the synthesis of DOM (Álvarez-Salgado et al. 1999), which is exported to the adjacent shelf during upwelling events and accumulated/consumed *in situ* during relaxation/downwelling events (Álvarez-Salgado et al. 2001). The present study, focused on the contribution of carbohydrates to the dissolved and suspended organic carbon pools, constitutes a step forward in our knowledge of the behaviour of DOM in this coastal upwelling system. We demonstrate the importance of carbohydrates for carbon cycling at the different stages of the seasonal cycle and examine the lability of this carbon pool using the mono- to polysaccharide ratio.

MATERIALS AND METHODS

Survey area. Fig. 1 shows the study area, comprising the Ría de Vigo and the adjacent shelf, the 2 contrasting domains sampled during the present study. On the one hand, the rías are characterised by a 2-layered residual circulation pattern, with an ongoing bottom current and an outgoing surface current during upwelling events, and a reversal of the flow during downwelling conditions. Therefore, these large (>2.5 km^3) V-shaped embayments respond to the influence of shelf winds despite being protected by island barriers (Gilcoto et al. 2001). In addition, continental runoff modulates the circulation of the rías, mainly at the innermost segment, which behaves as a partially mixed estuary driven by tidal currents (average tidal range, 3 m) and river runoff. In the case of the Ría de Vigo, the main tributary is the Oitabén-Verdugo river, which had an average flow of 18 m^3 s^{-1} during the study period.

On the other hand, the circulation of shelf waters off the Rías Baixas is more complex; it is composed of a wind-driven along-shore current and an across-shore exchange with the adjacent ocean and the Rías Baixas.

During the upwelling season, shelf surface waters are imported from the rías, and the bottom waters of the rías enter from the shelf. On the contrary, during the downwelling season, a convergence front between the shelf and the rías develops. The position of this front in the alongshore direction depends on the relative strength of coastal winds and continental runoff (Álvarez-Salgado et al. 2000).

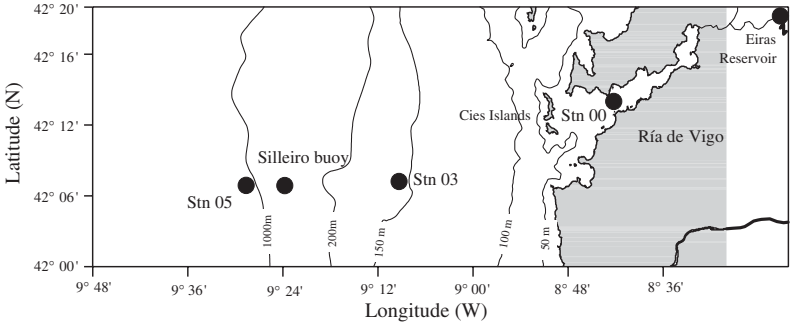

Fig. 1. The Ría de Vigo and adjacent shelf (NW Iberian Peninsula). The positions of the 3 stations are shown. The Eiras station at the upper course of the Oitabén-Verdugo river is also indicated

Sampling strategy. Two stations were sampled weekly from May 2001 to April 2002 from aboard the RV 'Mytilus'. The mid-shelf station (Stn 03; 42° 07.8' N, 9° 10.2' W, 150 m deep) was sampled from 08:00 to 10:00 h GMT. Station 00 (42° 13.8' N, 8° 51.0' W) was located in the middle segment of the Ría de Vigo (40 m deep in low water) and was sampled from 14:00 to 15:00 h GMT. Full-depth continuous conductivity-temperature-depth (CTD) profiles were recorded at each sampling site with a SBE 9/11 CTD device incorporated into a rosette sampler equipped with twelve 10 l Niskin bottles. Conductivity measurements were converted into practical salinity scale values (UNESCO 1985). Seawater samples were collected from 5, 25, 40, 60, 75, 100 and 150 m at Stn 03, and 5, 15 and 40 m at Stn 00. In addition, 2 samples of ENACW were taken at an oceanic station (Stn 05; 42° 07.8' N, 9° 30.0' W, 1200 m deep) at 150 and 200 m.

Aliquots for dissolved and particulate organic matter analyses were collected in 500 ml acid-cleaned glass flasks and 5 l acid-cleaned PVC containers, respectively. Dissolved organic matter samples were filtered through precombusted (450°C, 4 h) 47 mm ø Whatman GF/F filters in an acid-cleaned glass filtration system, under low N_2-flow pressure. Two aliquots were recovered for organic carbon (DOC) and carbohydrates (d-CHO). Samples for the analysis of DOC were collected in 10 ml precombusted (450°C, 12 h) glass ampoules. After acidification with H_3PO_4 to pH <2, the ampoules were heat-sealed and stored in the dark at 4°C until analysis. For d-CHO, the filtrate was collected in 50 ml polyethylene containers and frozen at –20°C until analysis. Suspended organic matter was collected under low-vacuum on precombusted (450°C, 4 h) 25 mm ø Whatman GF/F filters for organic carbon (POC, 0.5 to 1.5 l of seawater) and carbohydrates (p-CHO, 250 to 500 ml of seawater). All filters were dried overnight and frozen (–20°C) before analysis. Samples for DOC and POC were collected during every survey (weekly), whereas d-CHO and p-CHO were taken every 2 surveys (fortnightly).

In addition, 1 station in the upper course of the Oitabén-Verdugo river was sampled regularly during the seasonal cycle (Eiras reservoir, Fig. 1). Samples for DOC, POC, d-CHO and p-CHO were taken with a 1.7 l Niskin bottle, adapted for riverine samples, at the surface layer. They were processed as for the seawater samples.

Carbon analyses. DOC was measured with a commercial Shimadzu TOC-5000 organic carbon analyser, working under the principle of high-temperature catalytic oxidation. After decarbonation of the sample by vigorous stirring with high-purity synthetic air for 15 min, 200 µl were injected into the vertical furnace (a quartz tube) of the analyser, filled with a 0.5% Pt-coated Al_2O_3 catalyst at 680°C. This resulted in quantitative production of CO_2 from the DOC in the sample; and this CO_2 was measured in a Shimadzu infrared gas analyser. Three to 5 replicate injections were performed per sample and the system was standardised daily with potassium hydrogen phthalate in Milli-Q water. The concentration of DOC was determined by subtracting the average peak area from the instrument blank area and dividing by the slope of the standard curve. The system blank, obtained by frequent injection (every 5 samples) of UV-Milli-Q water, was equivalent to 5 to 10 µmol C l^{-1}. The precision of measurements was 1%, i.e. ±0.7 µmol C l^{-1}. Their accuracy was tested daily with the DOC reference materials provided by D. Hansell (University of Miami). We obtained an average concentration of 45.7 ± 1.6 µmol C l^{-1} (n = 26) for the deep ocean reference (Sargasso Sea deep water, 2600 m) minus blank reference materials. The nominal value provided by the reference laboratory was 44.0 ± 1.5 µmol C l^{-1}.

Measurements of POC were carried out with a Perkin Elmer 2400 CHN analyser. Filters were packed into 30 mm tin disks and injected into a vertical quartz furnace where combustion to CO_2, N_2 and H_2O was performed at 900°C. After separation of the gas products in a chromatographic column, a conductivity detector quantified the C, N and H content of the sample. Daily standards of acetanilide were added. The precision of the method was ±0.3 µmol l^{-1} for carbon.

Carbohydrate analyses. The determination of p-CHO carbohydrates was carried out using the anthrone method (Ríos et al. 1998). This is based on the quantitative reaction of sugars with anthrone in a strongly acidic medium at 90°C, giving an intensely coloured compound. The absorption was measured at 625 nm. To avoid manipulation of a strong acid (12M H_2SO_4), detection of the coloured compound was performed in a segmented flow analysis (SFA) system. It was necessary to use an all-glass manifold and a pump-tube of Viton® for the sample. The system was calibrated daily with D-glucose standards. The estimated accuracy of the method is ±0.1 µmol C l^{-1}.

Dissolved mono- and polysaccharides (MCHO and PCHO) were determined by oxidation of the free reduced sugars with TPTZ, followed by spectrophotometric analysis (Myklestad et al. 1997, Hung et al. 2001). Briefly, the redox reactions are as follows:

$$RCHO + 2Fe(CN)_6^{3-} + 3OH^- \rightarrow RCO_2 + 2Fe(CN)_6^{4-} + 2H_2O$$

$$2Fe(CN)_6^{4-} + TPTZ \rightarrow Fe(TPTZ)_2^{2+}$$
(violet-coloured complex)

The aldehydes of the MCHO or the PCHO (after hydrolysis of glycosidic bonds) are oxidised at alkaline pH; consequently, Fe^{3+} is reduced to Fe^{2+}. TPTZ is then condensed with the resultant Fe^{2+} to give a violet-coloured $Fe(TPTZ)_2^{2+}$ complex, which is spectrophotometrically determined at 595 nm. Hydrolysis of PCHO was carried out at pH = 1, at 150°C for 1 h. Samples were acidified with HCl and, after hydrolysis, were neutralised with NaOH. The reagents and products involved in the reactions are light sensitive; because of this, all the analytical procedure must be carried out in the dark. Due to the large number of samples and the sensitivity of the method to ambient light, the detection of the coloured compound was run in an automated SFA system. MCHO concentrations were quantified using a daily calibration curve made from D-glucose in Milli-Q water with concentrations between +0 and +32 µmol C l^{-1}, whereas the standardisation of d-CHO was made with D-glucose and soluble starch in Milli-Q water, at the same concentrations. Differences between calibration curves in Milli-Q water and seawater were negligible, as previously indicated by Witter & Luther III (2002). Quantification of MCHO and d-CHO was made by subtracting the average peak height from the blank height, and dividing by the slope of the standard curve. d-CHO values were corrected for dilution during the hydrolysis step. PCHO concentrations were calculated as the difference between d-CHO and MCHO. Three replicates were measured for each sample. The estimate accuracy was ±0.6 µmol C $l^{-1}$for MCHO and ±0.7 µmol C l^{-1} for d-CHO, and the detection limit was ~2 µmol C l^{-1}. Therefore, the calculated accuracy for PCHO was ±0.9 µmol C l^{-1} [$(0.6^2 + 0.7^2)^{0.5}$].

Meteorological variables. Daily Ekman transport values ($-Q_X$, m^2 s^{-1}) were calculated according to Wooster et al. (1976):

$$-Q_X = \frac{\rho_{air} \cdot C \cdot |V| \cdot V_y}{\rho_{SW} \cdot f} \quad (1)$$

where ρ_{air} is the density of air, 1.22 kg m^{-3} at 15°C; C is an empirical drag coefficient (dimensionless), 1.3 × 10^{-3}; f is the Coriolis parameter, 9.946 × 10^{-5} s^{-1} at 43° latitude; ρ_{SW} is the density of seawater, ~1025 kg m^{-3}; $|V|$ is the wind speed; and V_y is the north component of wind speed. Wind data were taken hourly from the anemometer of the SeaWatch Buoy, Silleiro Meteorological Observatory at 42° 07.2′ N, 9° 24.0′ W (www.puertos.es). Positive values indicate upwelling, and downwelling occurs when negative values are obtained.

Daily continental runoff (Q_R, m^3 s^{-1}) was estimated as the sum of a function of precipitation in the drainage basin, 589 km^2 (Ríos et al. 1992), and the flow from the Oitabén-Verdugo river, regulated by the Eiras reservoir.

Regression analysis. The best-fit between any variable couple (X, Y) was obtained minimising the function:

$$\sum_i \left[\left(X_i - \hat{X}_i\right)^{w_X} \times \left(Y_i - \hat{Y}_i\right)^{w_Y} \right]^2 \quad (2)$$

where w_X and w_Y are weights for X and Y respectively, with w_X, $w_Y \geq 0$ and $w_X + w_Y = 1$ and i denotes samples. The weight factors are a function of the estimated experimental error of the measured variable (er) regarding the standard deviation (SD) of the whole set of measurements of such variable. For a given couple of variables:

$$w_X = \left(\frac{er_X}{SD_X}\right) \Big/ \left(\frac{er_X}{SD_X} + \frac{er_Y}{SD_Y}\right); \; w_Y = 1 - w_X \quad (3)$$

Any regression model can be expressed as a linear combination of 2 extreme categories: (1) model I, which should be applied when $w_X = 0$, $w_Y = 1$ and (2) model II, when $w_X = w_Y = 0.5$ (Sokal & Rohlf 1995).

RESULTS

Dissolved and suspended CHO in relation to the hydrography of NW Spain

Seven hydrographic periods can be discerned on the basis of the seasonal evolution of key meteorological variables such as $-Q_X$ and Q_R (Fig. 2a, Table 1) and the observed water column response (Fig. 2b–e). The first

period, during spring and summer, was characterised by moderate upwelling-favourable winds separated by shorts intervals of wind calm. This caused marked summer stratification, with warm waters at the surface (17 to 19°C) and cold waters at the bottom (13°C). Average $-Q_X$ values indicated moderate upwelling ($-\bar{Q}_X = 257$ m^3 s^{-1} km^{-1}) and reduced continental runoff ($\bar{Q}_R$ = 15 m^3 s^{-1}). At the end of summer, a strong upwelling event ($-\bar{Q}_X$ = 500 m^3 s^{-1} km^{-1}) produced a sudden cooling of the water column: temperature in the surface layer decreased down to 15–16°C due to the uplift of ENACW (Fig. 2c). During October, continental runoff was high ($\bar{Q}_R$ = 47 m^3 s^{-1}) and coastal winds experienced a dramatic change in direction ($-\bar{Q}_X = -347$ m^3 s^{-1} km^{-1}) that promoted downwelling. This downwelling produced a reversal of the residual circulation of the ría (Fig. 2a) with an entry of warm oceanic surface water (Fig. 2c,e). From 20 to 22 October, strong runoff was observed (>300 m^3 s^{-1}, Fig. 2a) that restored the positive residual circulation pattern. A transition from stratification to vertical homogenisation occurred by 20 November, coinciding with enhanced Ekman transport values ($-\bar{Q}_X = 712$ m^3 s^{-1} km^{-1}) and low continental runoff ($\bar{Q}_R$ = 10 m^3 s^{-1}). At the end of autumn and the beginning of winter, a new wind reversal ($-\bar{Q}_X = -216$ m^3 s^{-1} km^{-1}) promoted the intrusion of the Iberian Poleward Current (IPC) to the shelf, characterised by a salinity maximum (Fig. 2d) and relatively warm temperatures >14°C (Fig. 2e). Continental runoff ($\bar{Q}_R$ = 13 m^3 s^{-1}) was perceptible only at the innermost station, where surface salinity decreased below 34.0 (Fig. 2b). Maximum vertical homogenisation occurred during the winter mixing period (by March), coinciding with positive values of $-\bar{Q}_X$ (231 m^3 s^{-1} km^{-1}) and limited runoff ($\bar{Q}_R$ = 17 m^3 s^{-1}). Finally, the beginning of the spring transition from homogenisation to stratification was observed at the end of the study period, with enhanced positive values of $-\bar{Q}_X$ (381 m^3 s^{-1} km^{-1}), reduced $\bar{Q}_R$ (10 m^3 s^{-1}) and a slight increase in surface temperature (Fig. 2c,e).

The position of the convergence front between the IPC and continental waters along the Ría de Vigo depends on the relative importance of $-Q_X$ and Q_R and Álvarez-Salgado et al. (2000) demonstrated that the residual circulation at Stn 00 could be explained with these 2 variables using the equation:

$$Q_{S00} = 16(\pm 4) \cdot 10^{-3} Q_R - 2.3(\pm 0.2) \cdot 10^{-3} Q_X \quad (4)$$

where Q_{S00} (10^3 m^3 s^{-1}) is the surface water flux at Stn 00 (Fig. 2a). Considering this flux and the volume of the ría from the inner waters to Stn 00 (0.53 km^3), renewal rates were estimated for every period (Table 1). Under summer stratification and upwelling conditions, the residual circulation was positive ($\bar{Q}_{S00}$ = 0.8 ± 0.1 and 1.3 ± 0.1 10^3 m^3 s^{-1}, respectively) with large renewal rates (13 ± 2 and 21 ± 2% d^{-1}). During the downwelling period, the flux virtually stopped ($\bar{Q}_{S00}$ = 0.0 ± 0.1 10^3 m^3 s^{-1}), because of enhanced runoff balancing the downwelling pattern, with a renewal of only 2 ± 2% d^{-1}. Larger renewal rates occurred during the transitional period (29 ± 3% d^{-1}). The average renewal rate for the study year was 9 ± 2% d^{-1}, and the residual circulation at Stn 00 remained positive at 0.6 ± 0.1 10^3 m^3 s^{-1}.

Period average concentrations of particulate organic matter, POC and p-CHO, at Stn 00 (Fig. 3a,b) showed maxima in surface waters during the summer stratification (48 and 11.0 µM C, respectively), and minima at 15 m during the transitional and poleward periods (10 and 0.4 µM C, respectively). In the mid-shelf station (Fig. 3c,d) maxima were located at the surface, during upwelling events for POC (14 µM C) and during summer stratification for p-CHO (1.8 µM C). Concentrations at the bottom were larger than at Stn 00, suggesting the existence of a bottom nepheloid layer due to resuspension of organic-rich sediments. The lowest concentrations were also found during the transitional and IPC periods. In general, there was a good agreement between POC and p-CHO distributions ($r = +0.88$, $p < 0.001$, $n = 298$).

Average POC and p-CHO (Stn 00, Fig. 4a,b; Stn 03, Fig. 5a,b) decreased monotonically with depth, although a significant rise was observed at the bottom layer ($p < 0.001$). Even though concentrations at the innermost station were higher than at the outermost one, the contribution of carbohydrates to POC was similar for both of them (14 ± 6%). The average profile of the p-CHO percentage showed a significant decrease ($p < 0.001$) with depth at Stn 00 (Fig. 5c). At Stn 03 (Fig. 6c) an absolute maximum at 75 to 100 m depth was observed. The slope of the correlation between p-CHO and POC (regression model II) was 0.26 ± 0.01 for Stn 00 and 0.12 ± 0.01 for Stn 03 (Table 2). This suggests that 26 ± 1% of the POC produced at the innermost station was p-CHO, whereas the percentage decreased down to 12 ± 1% at the mid-shelf station. The origin intercept, i.e. the fraction of p-CHO that did not co-vary with POC, represents the residual organic carbon that remained when p-CHO was zero. At Stn 00, this residual POC was about 1.8 ± 0.2 µM C (11% of average POC at Stn 00), but the origin intercept at Stn 03 was not significant.

Surface accumulation of DOC occurred during the downwelling and summer stratification periods (>90 µM C) and the upwelling period (90 µM C) at Stn 00, and during the summer stratification, upwelling and spring periods (70 to 90 µM C) and the downwelling period (70 µM C) at Stn 03 (Fig. 6a,d). Relatively high average DOC values were found at 100 and 150 m at the outermost station during the IPC

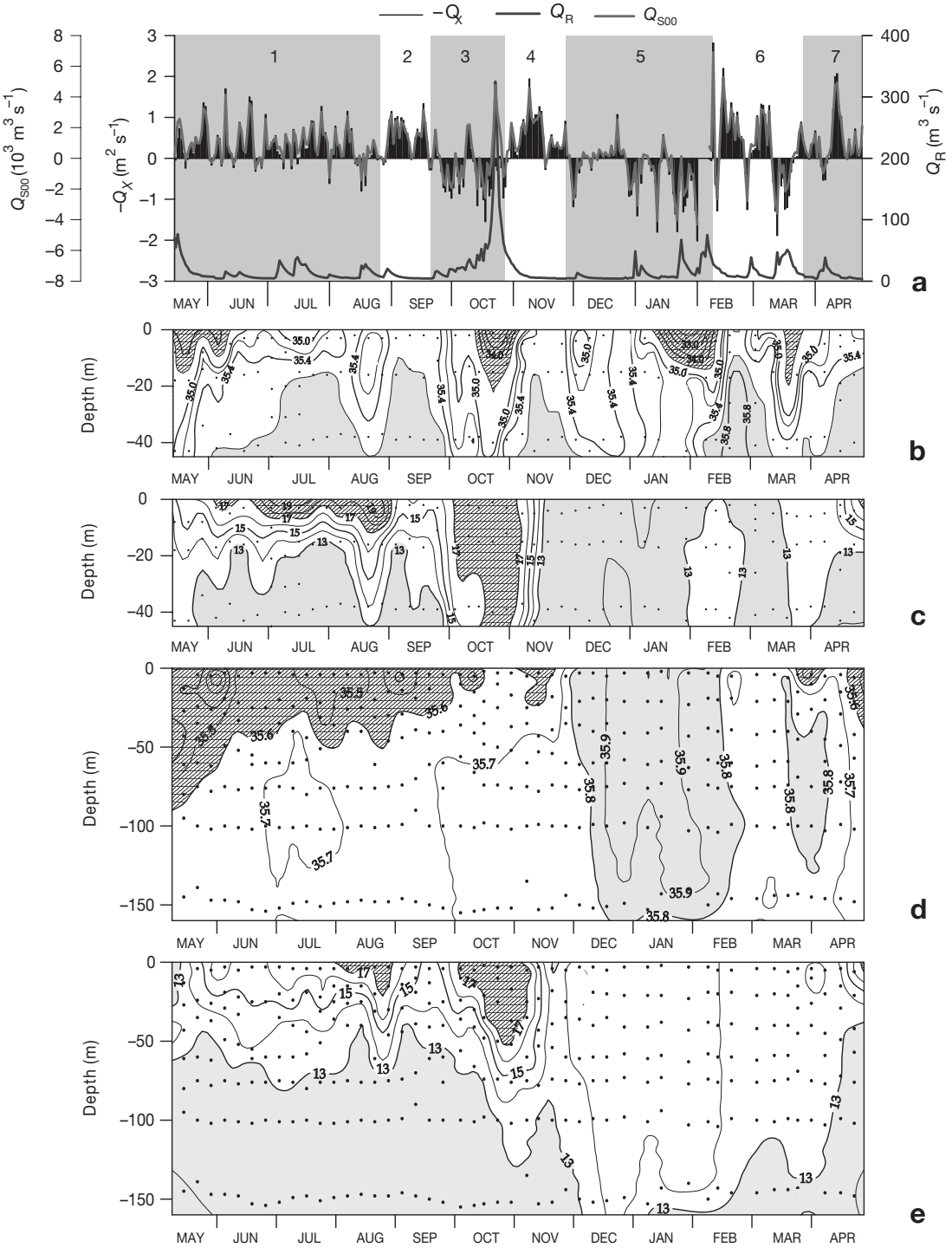

Fig. 2. Time course of (a) Ekman transport, $-Q_X$ ($m^2\ s^{-1}$), continental runoff, $-Q_R$ ($m^3\ s^{-1}$) and surface water flux at Stn 00 (Q_{S00}, $10^3\ m^3\ s^{-1}$), (b) salinity at Stn 00, (c) temperature (°C) at Stn 00, (d) salinity at Stn 03 and (e) temperature (°C) at Stn 03. The 7 different hydrographic periods are shown in (a) and Table 1

period. Average minima occurred in bottom waters and for the periods of transition and winter mixing. During the period of enhanced runoff in October, large concentrations were observed throughout the water column at Stn 00. DOC correlated well with salinity and temperature ($r = +0.77$, $p < 0.001$, $n = 298$), indicating that mixing of water masses was a process relevant to DOC distributions.

The time evolution of d-CHO was similar to that of DOC (r = +0.81, p < 0.001, n = 298), with surface maxima when the water column was stratified and during the downwelling period due to the high runoff (17 and 12 µM C at Stn 00 and 03, respectively), and lower values at deeper layers. This pattern was also observed in PCHO (Fig. 6b,e). In contrast, the distribution of MCHO (Fig. 6c,f) was more homogeneous and showed lower concentrations. d-CHO and PCHO correlated significantly with temperature and salinity (r = +0.69, p < 0.001, n = 298 and r = +0.67, p < 0.001, n = 298, respectively).

Table 1. Average offshore Ekman transport ($-\bar{Q}_X$, $m^2\ s^{-1}$), continental runoff ($\bar{Q}_R$, $m^3\ s^{-1}$), surface water flux at Stn 00 ($\bar{Q}_{S00}$, $10^3\ m^3\ s^{-1}$) and renewal rate at Stn 00 (% d^{-1}) for the 7 hydrographic periods identified during the sampling period. Positive $-\bar{Q}_X$ values indicate upwelling, negative values downwelling. Positive Q_{S00} values indicate a positive residual circulation pattern and negative values a negative residual circulation pattern. For $\bar{Q}_{S00}$ and renewal rate the errors associated with Eq. (4) are shown

	Period	Date	$-\bar{Q}_X$	$\bar{Q}_R$	$\bar{Q}_{S00}$	Renewal rate
1	Summer strat.	15 May–21 Aug	257	15	0.8 ± 0.1	13 ± 2
2	Upwelling	28 Aug–18 Sep	500	8	1.3 ± 0.1	21 ± 2
3	Downwelling	25 Sep–30 Oct	−347	47	0.0 ± 0.1	2 ± 2
4	Transition	6 Nov–20 Nov	712	10	1.8 ± 0.2	29 ± 3
5	IPC	27 Nov–13 Feb	−216	13	−0.3 ± 0.1	5 ± 1
6	Winter mixing	20 Feb–26 Mar	231	17	0.8 ± 0.1	13 ± 2
7	Spring	2 Apr–24 Apr	381	10	1.0 ± 0.1	17 ± 2
	Annual cycle	15 May–24 Apr	129	17	0.6 ± 0.1	9 ± 2

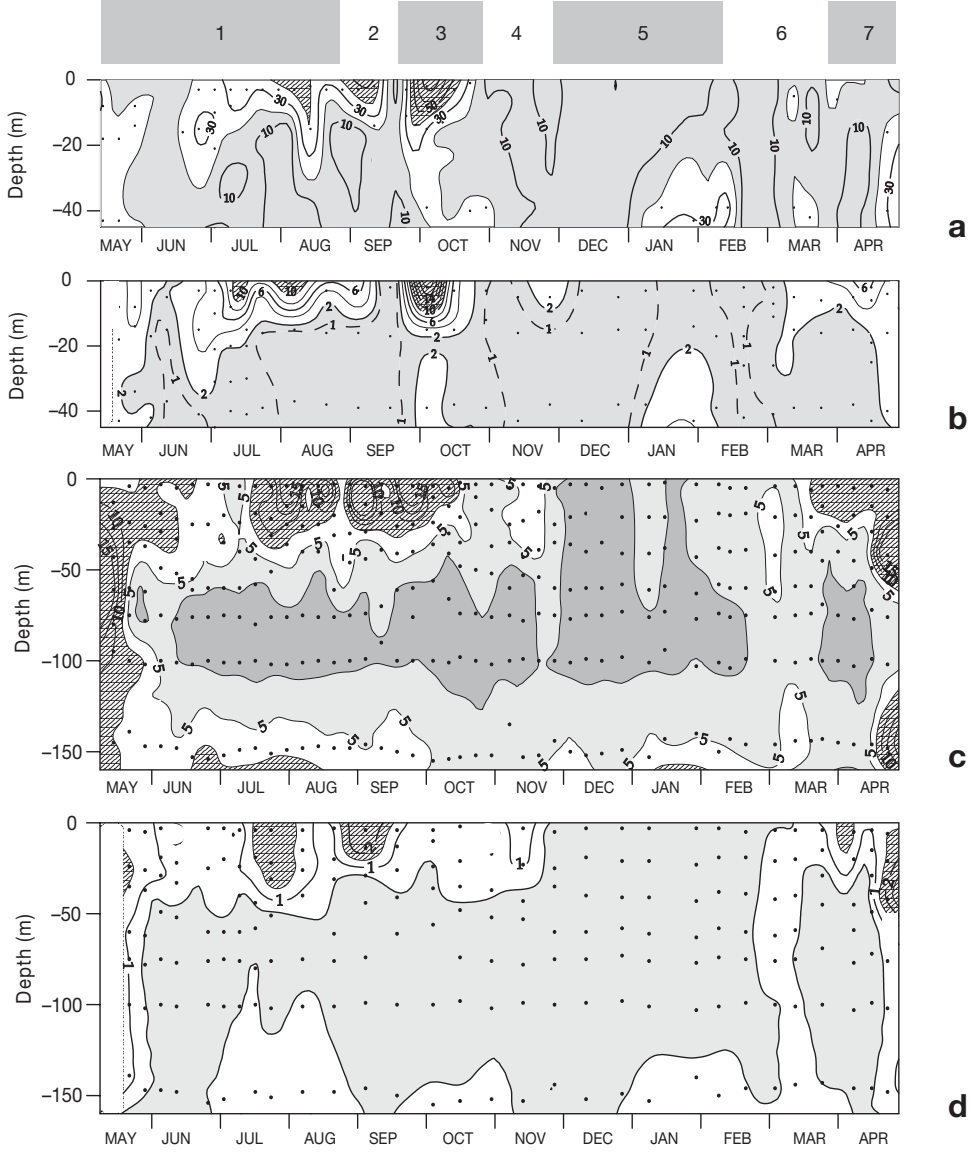

Fig. 3. Time course of (a) POC (µM C) at Stn 00, (b) p-CHO (µMC) at Stn 00, (c) POC (µM C) at Stn 03 and (d) p-CHO (µMC) at Stn 03 during the study period

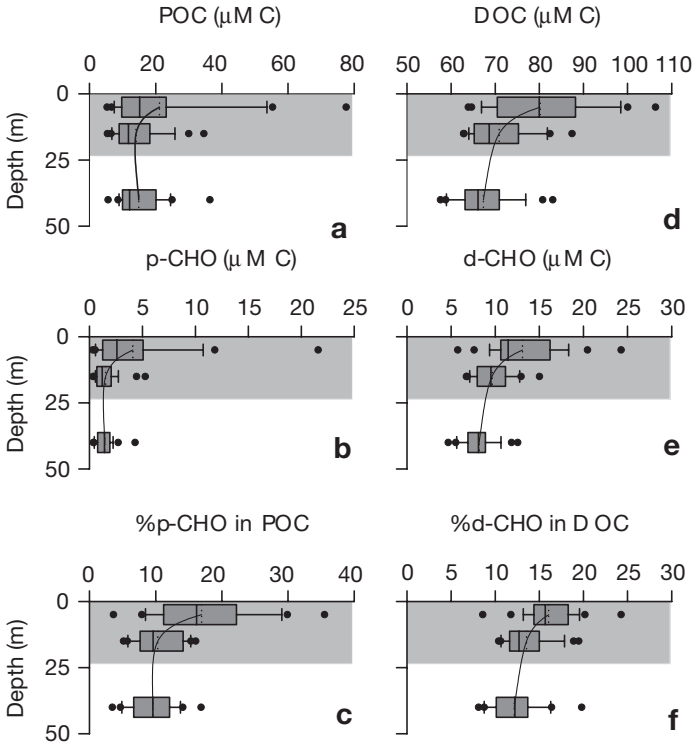

Fig. 4. Box and whisker plot of (a) POC (µM C), (b) p-CHO (µM C), (c) % p-CHO in POC, (d) DOC (µM C), (e) d-CHO (µM C) and (f) % d-CHO in DOC for the whole data set at Stn 00. Fifty percent of the data are included within the limit of the boxes and the caps represent the 10th and 90th percentiles. Solid lines represent the average profiles. Shadowing symbolises the average photic layer

The average DOC and d-CHO profiles (Stn 00, Fig. 4d,e) displayed the expected maximum values at the surface and decreased significantly with depth ($p < 0.001$). The same pattern was observed at Stn 03 (Fig. 5d,e), but in this case with lower concentrations and less variability in the upper layer. Typical DOC and d-CHO values found at Stn 00 varied from 80 and 13 µM C at the surface layer to 65 and 8 µM C at the bottom, respectively. On average, d-CHO made up 13 ± 3% of DOC, showing higher values at the surface layer that decreased significantly ($p < 0.001$) with depth (Fig. 4f, Stn 00 & Fig. 5f, Stn 03).

d-CHO variability can be explained as a linear combination of temperature and DOC [regression model I for temperature (T) and combination of regression models I and II with $w_Y = 0.8$ for DOC; $r = +0.82$, $p < 0.001$ at Stn 00 and $r = +0.79$, $p < 0.001$ at Stn 03; Table 2]. Fig. 7c shows the covariation between d-CHO and DOC anomalies, calculated as: $aY = Y - a_0 - a_1T$ (where a_0 and a_1 are the coefficients of the linear multiple regression of Y with temperature). These anomalies (*a* d-CHO from correlation of d-CHO vs T in Fig. 7a, and *a* DOC from correlation of DOC vs T in Fig. 7b) only retained the variability associated to the biogeochemical processes. Therefore, these multiple regressions explain the changes of dissolved carbohydrates as a function of water masses mixing (T) and biogeochemistry (DOC). The d-CHO/DOC slope, independent of water masses mixing, indicated that d-CHO represented 29 ± 4% of the net production of DOC at Stn 00; this value was not significantly different from the obtained at Stn 03 (31 ± 4%, Table 2).

A carbohydrate budget for the NW Iberian upwelling

A rough estimation of the surface carbon excess can be performed with a simple 2-endmember mixing model, one endmember being the freshwater input (F), and the other endmember the bottom water at the study site. For DOC we can write:

$$\Delta DOC = DOC_S - \left(\frac{S_B}{S_B} \cdot DOC_B + \frac{S_B - S_B}{S_B} \cdot DOC_F \right) \quad (5)$$

where ΔDOC is the surface DOC excess, DOC_S and S_S are the DOC and salinity in the surface layer, DOC_B and S_B are the DOC and salinity at the bottom, and DOC_F is the DOC in the continental runoff. The same equation can be written for POC, p-CHO, d-CHO, PCHO and MCHO, and for the 2 study sites. The Oitabén-Verdugo river is the freshwater end-member, considering the concentrations obtained at the Eiras reservoir (S = 0.00).

Seasonal accumulation of POC (ΔPOC) was higher at the innermost station (6.5 and 4.2 µM C at Stns 00 and 03, respectively). The same occurred with seasonal accumulation of particulate carbohydrates (Δp-CHO) with 2.5 µM C at Stn 00 and 0.2 µM C at Stn 03, implying that ~40% of the POC accumulated at Stn 00 consists of carbohydrates, but just ~6% at the mid-shelf station.

As mentioned previously, a DOM excess was observed in surface waters, compared to bottom waters, at the 2 sites throughout the study period. The average excesses for Stn 00 were 10.8 and 4.5 µM C of DOC and d-CHO, respectively. In the case of Stn 03, ΔDOC and Δd-CHO (seasonal accumulation of dissolved carbohydrates) were 8.3 and 2.7 µM C, respectively. The carbohydrate percentage in this fraction was 42% for the innermost station, whereas at the mid-shelf station the value was lower (33%). The DOM accumulation depended on the hydrographic conditions; the excess was maximal during the upwelling period (18.8 and 7.5 µM C for DOC and d-CHO, Stn 00) and minimal during the winter mixing period (1.9 and 0.3 µM C for

DOC and d-CHO, Stn 00). At Stn 03 the excess was lower and less variable. The highest accumulations occurred during the summer stratification and upwelling, and they were minimal during the IPC period.

Calculated renewal rates for Stn 00 allowed estimation of the net production of the inner Ría de Vigo. On average 1.0 µmol C l^{-1} d^{-1} of DOC and 0.4 µmol C l^{-1} d^{-1} of d-CHO, were produced. During the maximum accumulation period (upwelling) 3.9 and 1.6 µmol C l^{-1} d^{-1} of DOC and d-CHO, were produced. In the period of winter mixing (lower accumulation) the estimated production was only 0.3 and 0.1 µmol C l^{-1} d^{-1}.

Correlation of TOC (total organic carbon) with *T* and POC (regression model I for *T*, combination between regression models I and II with $w_Y = 0.4$ at Stn 00 and $w_Y = 0.2$ at Stn 03 for POC; Table 2) showed different results at the 2 study sites. Every mole of POC generated 0.4 ± 0.1 moles of DOC at Stn 00 and 0.8 ± 0.1 moles at Stn 03. A similar calculation for t-CHO (total carbohydrates), *T* and p-CHO (regression model I for *T*, regression model II for p-CHO at Stn 03 and combination between regression models I and II with $w_Y = 0.7$ for p-CHO at Stn 00; Table 2) indicated larger differences between both locations. One mole of p-CHO produced 0.6 ± 0.1 moles of d-CHO in Stn 00, whereas it made 3.7 ± 0.5 moles of d-CHO at Stn 03.

Mono- to polysaccharide ratio of d-CHO

The average percentage of monosaccharides in d-CHO (Fig. 8a,b) increased slightly but significantly with depth ($p < 0.001$) at the 2 study sites. Similar average values were obtained for the 2 stations (30 to 40% MCHO), whereas in river samples the percentage of MCHO was higher and more variable (~50%, Fig. 8c). Correlation of PCHO and d-CHO (regression model II, Table 2) provided a slope of 0.82 ± 0.02 at Stn 00 and 0.87 ± 0.02 at Stn 03, which indicated that less than 20% of the d-CHO variation was due to MCHO.

The mono- to polysaccharide ratio in Δd-CHO was very low in both stations: MCHO accounted for 14 to 18% of Δd-CHO. The production rate at Stn 00 was 0.1 and 0.4 µmol C $l^{-1}d^{-1}$ of MCHO and PCHO, respectively. Higher average percentages of ΔMCHO were found in the periods of lower DOM accumulation (during winter mixing and spring). Higher production occurred during the upwelling period at the innermost station, 0.2 and 1.5 µmol C l^{-1} d^{-1} of MCHO and PCHO, respectively.

The freshwater endmember presented higher DOC and d-CHO concentrations than seawater samples: 91.1 and 47.9 µM C, respectively (1.1 and 3.6 times the values of the surface layer at Stn 00). It is noticeable that the MCHO concentration, 23.5 µM C, was 5.5 times higher than at Stn 00. Particulate material was also more abundant at the Eiras reservoir than at Stn 00: 49.0 µM C for POC (2.1 times higher) and 13.6 µM C for p-CHO (3.2 times higher).

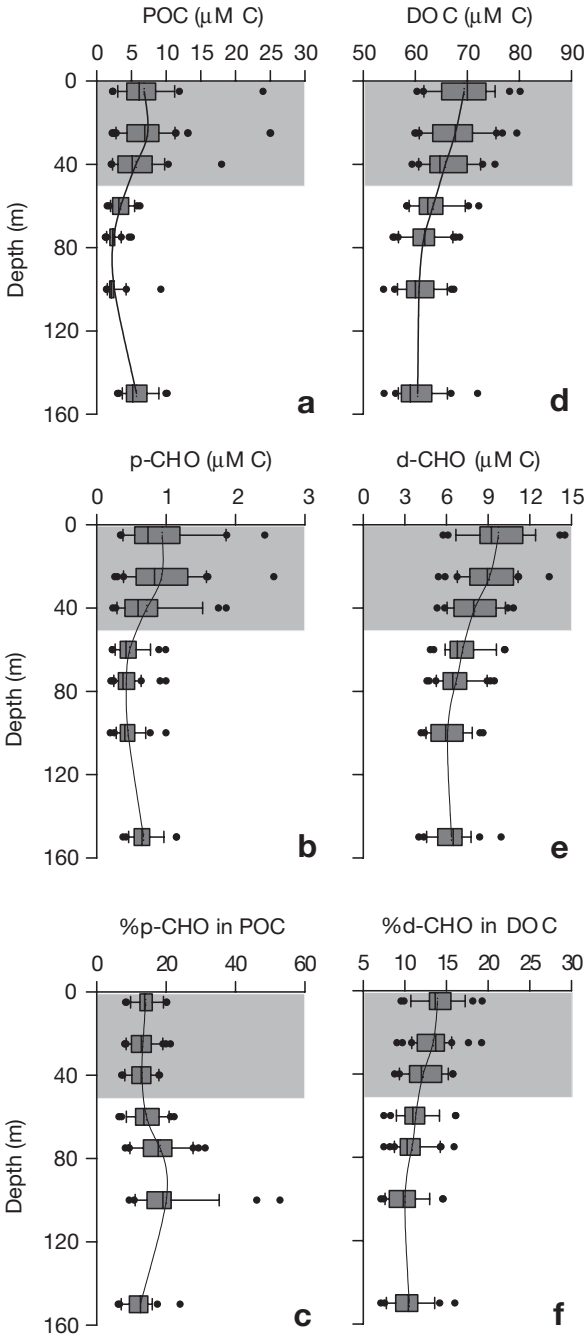

Fig. 5. Box and whisker plot of (a) POC (µM C), (b) p-CHO (µM C), (c) % p-CHO in POC, (d) DOC (µM C), (e) d-CHO (µM C) and (f) % d-CHO in DOC for the whole date set at Stn 03. Fifty percent of the data are included within the limit of the boxes and the caps represent the 10th and 90th percentiles. Solid lines represent the average profiles. Shadowing symbolises the average photic layer

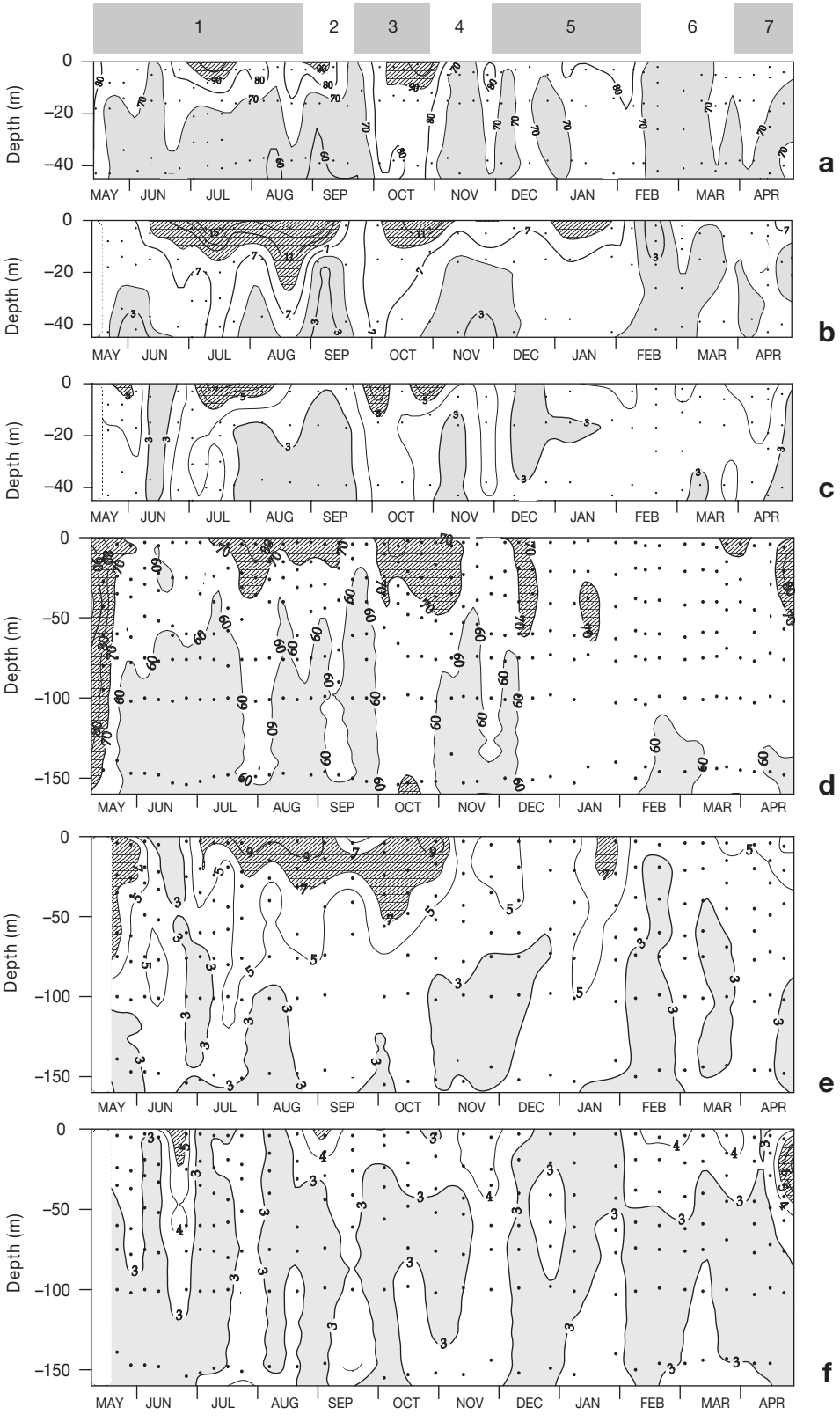

Fig. 6. Time course of (a) DOC (µM C) at Stn 00, (b) PCHO (µMC) at Stn 00, (c) MCHO (µMC) at Stn 00, (d) DOC (µM C) at Stn 03, (e) PCHO (µM C) at Stn 03 and (f) MCHO (µM C) at Stn 03 during the study period

Table 2. Selected significant ($p < 0.001$) linear regressions among physical and biogeochemical variables: particulate carbohydrates (p-CHO), particulate organic carbon (POC), dissolved carbohydrates (d-CHO), dissolved organic carbon (DOC), total carbohydrates (t-CHO), total organic carbon (TOC), dissolved polysaccharides (PCHO) and temperature (*T*). Numbers in brackets are the standard error of the coefficients; r = regression coefficient; n = number of samples

Station	Variables	Equation	r	n
p-CHO vs POC	Stn 00	p-CHO = –1.8 (±0.2) + 0.26 (±0.01) POC	+0.88	97
	Stn 03	p-CHO = 0.08 (±0.03) + 0.12 (±0.01) POC	+0.86	201
d-CHO vs *T*, DOC	Stn 00	d-CHO = –16 (±4) + 0.4 (±0.1) *T* + 0.29 (±0.03) DOC	+0.82	97
	Stn 03	d-CHO = –16 (±4) + 0.3 (±0.1) *T* + 0.31 (±0.04) DOC	+0.71	201
TOC vs *T*, POC	Stn 00	TOC = 22 (±6) + 3.1 (±0.5) *T* + 1.4 (±0.1) POC	+0.93	97
	Stn 03	TOC = 21 (±3) + 2.8 (±0.2) *T* + 1.8 (±0.1) POC	+0.86	201
t-CHO vs *T*, p-CHO	Stn 00	t-CHO = –4 (±2) + 0.9 (±0.2) *T* + 1.6 (±0.1) p-CHO	+0.90	97
	Stn 03	t-CHO = –5 (±1) + 0.8 (±0.1) *T* + 4.7 (±0.5) p-CHO	+0.75	201
PCHO vs d-CHO	Stn 00	PCHO = –1.8 (±0.2) + 0.82 (±0.02) d-CHO	+0.96	97
	Stn 03	PCHO = –1.8 (±0.2) + 0.87 (±0.02) d-CHO	+0.92	201

DISCUSSION

Hydrographic control of carbohydrate accumulation

Our results corroborate that seasonal DOC accumulation is closely connected with stratification, as was proposed by Carlson et al. (1994) for temperate, subpolar and continental shelf regions that exhibit convective mixing and spring re-stratification. The conspicuous succession of wind stress/relaxation cycles that occurs off the NW Iberian Peninsula is the reason behind the large productivity of this system and has a great influence on DOC cycling. Nutrient entry to the photic layer takes place during the 'spin-up' phase of upwelling events, whereas phytoplankton growth and accumulation happens during the 'spin-down' phase. DOM accumulation occurs after the bloom, accompanying phytoplankton decay. This hydrographic control of growth and accumulation of phytoplankton is a common phenomenon in coastal, upwelling systems at temperate latitudes (Barber & Smith 1981, Zimmerman et al. 1987). DOC accumulation at the end of blooms, during the period of relaxation, also seems to be quite a general pattern (Kirchman et al. 1994, Norrman et al. 1995, Chen et al. 1996, Doval et al. 1997), and in this study it was demonstrated that accumulation of carbohydrates follow the same pattern. Information about seasonal accumulation of carbohydrates is scarce, but Williams (1995) found evidence for the seasonal accumulation of dissolved carbon-rich materials, from mid to late summer. This work corroborates that these substances were carbohydrates, which make up 29 to 31% of the DOC changes in the water column and 33 to 42% of the DOC accumulation in seasonal thermocline waters.

The observed presence at the mid shelf of relatively warm (>14°C) and salty (>35.8) water all over the water column from December to February is due to the presence of the IPC. This IPC transports aged and remineralised subtropical waters, with low DOC, POC,

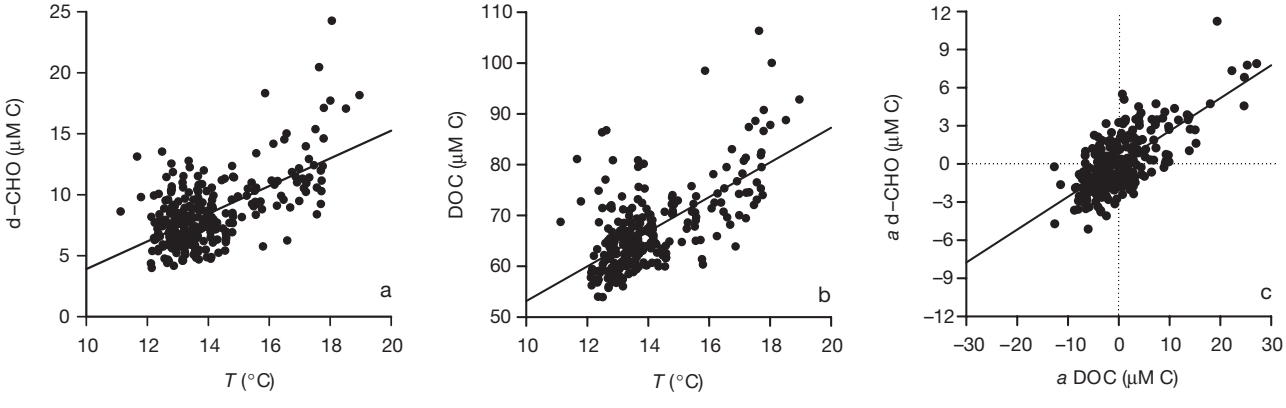

Fig. 7. (a) d-CHO versus *T*, (b) DOC versus *T* and (c) anomaly of d-CHO (*a* d-CHO) versus anomaly of DOC (*a* DOC). Solid lines represent the corresponding regression lines (model II; Sokal & Rohlf, 1995). Concentrations are in µMC and *T* in °C

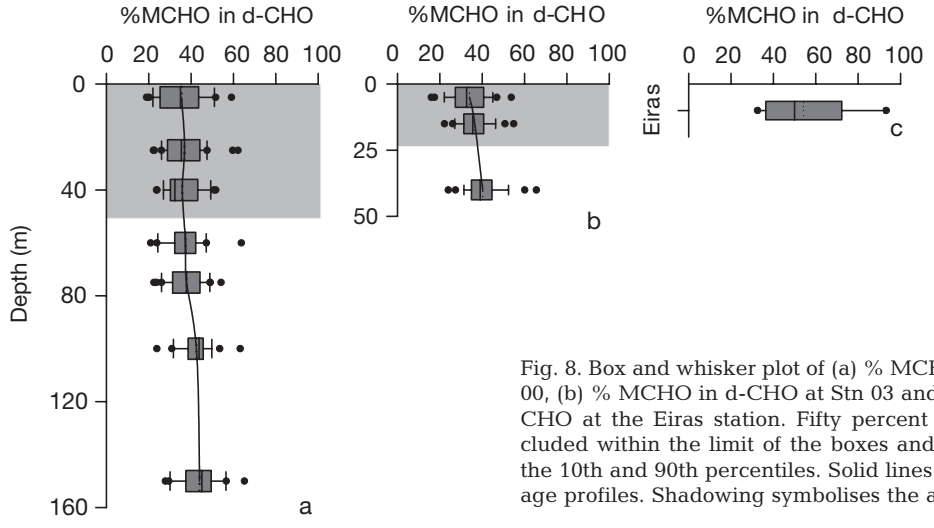

Fig. 8. Box and whisker plot of (a) % MCHO in d-CHO at Stn 00, (b) % MCHO in d-CHO at Stn 03 and (c) % MCHO in d-CHO at the Eiras station. Fifty percent of the data are included within the limit of the boxes and the caps represent the 10th and 90th percentiles. Solid lines represent the average profiles. Shadowing symbolises the average photic layer

d-CHO and p-CHO concentrations, to these latitudes. However, relatively high values of organic matter were found in the bottom waters of Stn 03 (100 and 150 m) during the IPC period, probably resulting from offshore export from the bottom ría under conditions of negative residual circulation. During winter, low and homogeneous concentrations of DOM and POM were observed, due to reduced primary production (<0.2 g C m^{-2} d^{-1}; Álvarez-Salgado et al. 2003).

As indicated in previous studies in the Rías Baixas (Fraga & Vives 1961, Fraga 1967, Doval et al. 1997), the high concentrations of POM in bottom waters can be due to the sedimentation of phytoplankton blooms, resuspension of organic-rich sediments or zooplankton accumulation. This bottom nepheloid layer has been recurrently observed in the Iberian upwelling (McCave & Hall 2002) and in other coastal regions (e.g. Sherwood et al. 1994). It was noticeable that p-CHO follows the same pattern as POC in the ría. However, at the middle shelf, the percentage of carbohydrate was lower at the bottom than at 75 to 100 m. This pattern could be explained on the basis of a fractionated mineralisation of sinking POM, with N- and P-rich compounds being preferentially mineralised at mid depths and carbohydrates at the bottom layers (Ríos et al. 1998).

The role of carbohydrates in the carbon balance of a marine ecosystem

The range of d-CHO concentrations at Stn 00 was similar to those provided by Hung et al. (2003) for the Gulf of Mexico (4 to 22 µM C) or by Witter & Luther III (2002) for the US Middle Atlantic Bight (3 to 17 µM C). However, concentrations of d-CHO were lower at Stn 03 and closer to the oceanic values provided by Pakulski & Benner (1994).

The contribution of p-CHO to the POC pool was ~15% for both stations, a value halfway between those presented by Hung et al. (2003) for the Gulf of Mexico (18% for 2000 and 9% for 2001). On the other hand, d-CHO accounted for 13 ± 3% of DOC, very close to the mean values provided by Pakulski & Benner (1994) for the North Atlantic Ocean (15 ± 2%) and by Børsheim et al. (1999) for the Trondheimsfjord (16 ± 2%). It has been widely confirmed that the percentage is higher at the surface layers (14 to 16% in this study).

Correlations between p-CHO and POC gave different results for both stations. At the outermost station only 12 ± 1% of the POC produced was p-CHO and the origin intercept was nearly zero, i.e. no residual carbon material remains when p-CHO is zero. Similar results were published by Hung et al. (2003) for the Gulf of Mexico: 18 ± 1 and 8.7 ± 0.4% in 2000 and 2001, respectively, with origin intercepts not significantly different from zero. However, the situation at Stn 00 was different: the contribution of p-CHO to POC was higher (26 ± 1%). In addition, there was a more persistent POC pool than p-CHO that accounted for 1.8 ± 0.2 µM C. These results agree with the calculated accumulations, higher in both cases (POC and p-CHO) at the innermost station, and richer in carbohydrates. This suggests that the interior of the ría is the most productive sector, exporting particulate matter to the adjacent shelf and the ocean. The lower percentage of p-CHO at the mid shelf station points to the existence of degradation and sinking processes during offshore transport, especially in the carbohydrate pool.

There is no significant difference in the carbohydrate portion in the freshly dissolved material between

the ría and the shelf (29 to 31%). These values are larger than the results obtained by Hung et al. (2003) in the Gulf of Mexico (21%), but they are similar to those proposed by Børsheim et al. (1999) for 2 coastal stations in the Trondheimsfjord (28 to 30%) and by Pettine et al. (1999) for the northern Adriatic Sea (30%). It has been demonstrated that d-CHO covaries with DOC in accordance with the time scale of the sampling frequency (2 wk).

Average ΔDOC in the middle of the ría was 11 µM, but during the upwelling period this value increased up to 19 µM, similar to that provided by Doval et al. (1997) for the same station during the 1995 upwelling season (21 µM). Carbohydrates composed a larger percentage at the innermost station: 42% compared with 33% at the shelf station. During the upwelling event, when offshore export is the most important physical process, the percentages were more similar: 38 and 36%, respectively. Estimations of the production at the innermost station gave higher values during this upwelling event (3.9 and 1.6 µmol C l^{-1} d^{-1} for DOC and d-CHO, respectively), 10 times those calculated during winter mixing (0.3 and 0.1 µmol C l^{-1} d^{-1}, respectively). To our understanding, no carbohydrate production data have been previously published. In the case of DOC, our value is comparable with that obtained by Doval et al. (1997) for the same study area during the upwelling season (4.2 µmol C l^{-1} d^{-1}).

Fig. 9 presents a tentative partitioning of the DOC pools at Stn 00 into surface and bottom waters. ENACW provides a major part of the DOC. This water mass contains minimum proportions of d-CHO (only 9% of DOC). The main d-CHO contributions are from the riverine input (53% of DOC) and, especially, new production (43%).

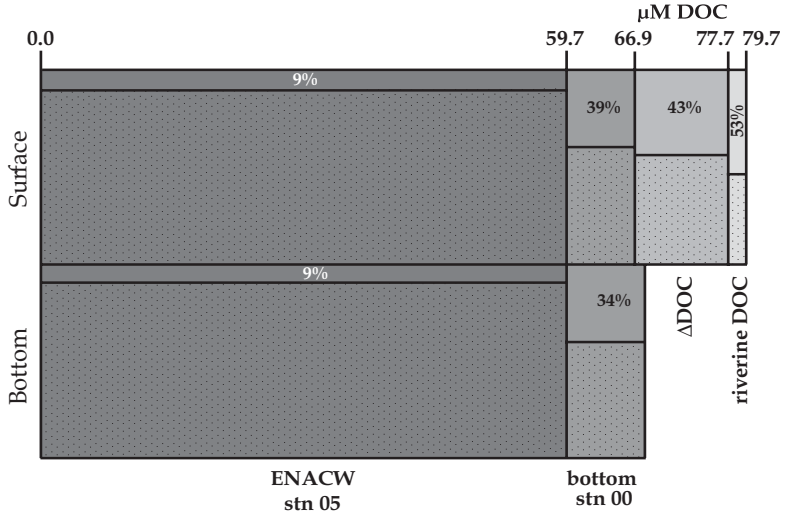

Fig. 9. Tentative partitioning of DOC at Stn 00 in surface and bottom waters during the seasonal cycle. % of d-CHO are indicated

As mentioned previously, good correlations were found between TOC and POC, and between t-CHO and p-CHO (Table 2). The slopes for both data sets give different results: 1 mole of POM generates more DOM at the middle shelf. However, differences are more notable for carbohydrates. Values are higher at the outermost station because dissolved materials are preferentially exported horizontally, whereas particulate materials preferentially sink to the bottom. In addition, waters in the middle ría are mesotrophic, whereas at the middle shelf they are more oligotrophic, leading to a preferential accumulation of dissolved carbohydrates (Williams 1995).

Lability of DOM

The slight increase in the contribution of MCHO to d-CHO with depth, and the average values of 30 to 40% observed during the study period, have been described before (Pakulski & Benner 1994, Hung et al. 2001). These works also report the nearly uniform (~4 µM C) vertical distribution of MCHO at many locations (3 ± 1 µM C in this study). Williams & Gray (1970) have hypothesised that MCHO and other low-molecular-weight organic substrates are rapidly assimilated to low concentrations by bacteria. This assumption is in accordance with the consideration of MCHO as an indicator of lability.

Percentages of MCHO in Δd-CHO were much lower (14 to 18%) than in the bulk d-CHO (30 to 40%), suggesting again the preferential accumulation of semi-labile PCHO rather than labile MCHO. The percentage of accumulated MCHO increased during the periods of low accumulation, but this was not due to enhanced MCHO but to depressed PCHO production. In all cases, the most productive period for both carbohydrate pools was the upwelling event.

The time course of PCHO throughout the study period was similar to that of d-CHO, and they correlate significantly. The slope of the correlations (regression model II) indicates that about 82% at Stn 00 and 87% at Stn 03 of the d-CHO change was due to PCHO.

Freshwater inputs have organic matter loads higher than the inner- and outermost stations, but the largest differences were found in carbohydrates. The p-CHO contribution to POC increases up to 32%, but the contribution of d-CHO to DOC is more remarkable, nearly 50% on average during the study period. Studies carried out in estuaries indicate the major contribution of

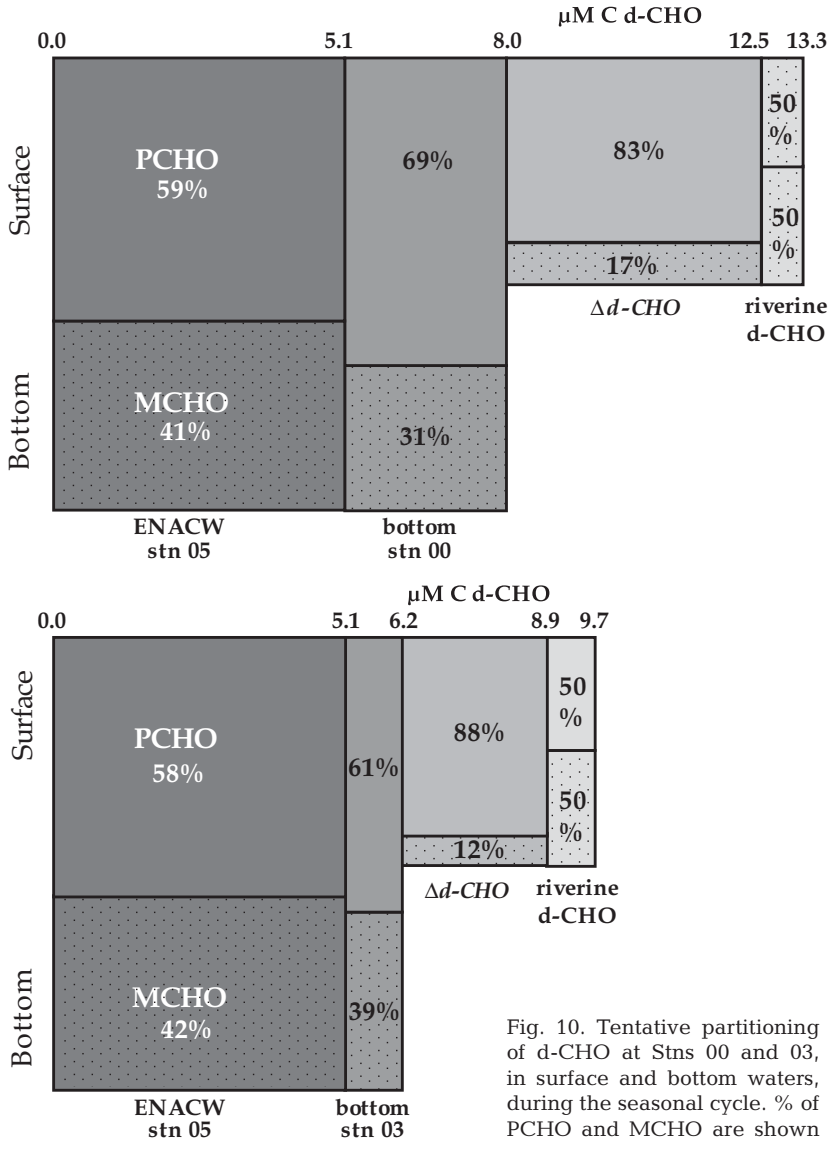

Fig. 10. Tentative partitioning of d-CHO at Stns 00 and 03, in surface and bottom waters, during the seasonal cycle. % of PCHO and MCHO are shown

carbohydrates to the C pool of rivers (Senior & Chevolot 1991, Hung et al. 2001, Witter & Luther III 2002). The degree of polymerisation of these sugars is different from the d-CHO pool in seawater: the percentage of MCHO increases in riverine waters (30 to 90%), in accordance with others authors, such as Senior & Chevolot (1991),who presented values ranging from 15 to 90% in the Elorn Estuary (Brest, France).

Fig. 10 presents the different dissolved carbohydrate pools calculated for the 2 different study sites, and the PCHO/MCHO contributions. The degree of polymerisation gives an idea of the lability of the material; semi-labile materials (81 to 88% PCHO) compose d-CHO accumulations, whereas riverine material is more labile (51% PCHO). Similar proportions of MCHO were found in both sites, but with higher concentrations at the innermost station.

Conclusions

Carbohydrates in the NW Iberian coastal upwelling system follow the same seasonal pattern as the organic carbon pool, being strongly influenced by physical and biological processes. Phytoplankton growth and POM accumulation (both POC and p-CHO) were observed during the upwelling period, whereas DOM (DOC and d-CHO) accumulated during the relaxation of the upwelling pulse, when phytoplankton biomass begins to decay.

Negative residual circulation dominated during the IPC period, with low values of DOM and POM except in the bottom layers at the mid shelf.

The surface excess of DOC is richer in carbohydrates than the bulk DOC. The percentage increases from 12–14% in DOC to 33–42% in ΔDOC, indicating that d-CHO is a major component of the freshly produced material in comparison with aged ENACW, where only 9% of DOC is d-CHO.

The surface Δd-CHO presents a higher percentage of PCHO than the rest of the d-CHO pool: 80 to 90% of the carbohydrate excess consists of polysaccharides, suggesting that the material is essentially semi-labile.

Acknowledgements. The authors wish to thank the captain and crew of the RV 'Mytilus' and the members of Oceanoloxía from the Instituto de Investigacións Mariñas and GOFUVI from the Universidade de Vigo for their inestimable help. Special thanks to T. Rellán for POC and p-CHO analysis, J. Gago for DOC analysis and J. L. Cortijo and S. Piedracoba for the meteorological data. Financial support for this work came from CICYT grant numbers MAR1999-1039-C02-01 and REN2000-0880-C02-01, and XUGA grant number PGIDT01MAR40201PN. A fellowship from the Spanish Ministerio de Ciencia y Tecnología funded M.N.-C. to carry out this work.

LITERATURE CITED

Aluwihare LI, Repeta DJ, Chen RF (1997) A major biopolymeric component to dissolve organic carbon in sea water. Nature 387:166–169

Álvarez-Salgado XA, Doval MD, Pérez FF (1999) Dissolved organic matter in shelf waters off the Ría de Vigo (NW Iberian upwelling system). J Mar Syst 18:383–394

Álvarez-Salgado XA, Gago J, Míguez BM, Gilcoto M, Pérez FF (2000) Surface waters of the NW Iberian margin: upwelling on the shelf versus outwelling of upwelled waters from the Rías Baixas. Est Coast Shelf Sci 51: 821–837

Álvarez-Salgado XA, Gago J, Míguez BM, Pérez FF (2001) Net ecosystem production of dissolved organic carbon in a coastal upwelling system: the Ría de Vigo, Iberian margin of the North Atlantic. Limnol Oceanogr 46:135–147

Álvarez-Salgado XA, Figueiras FG, Pérez FF, Groom S and 10 others (2003) The Portugal coastal counter current off NW Spain: new insights on its biogeochemical variability. Prog Oceanogr 56:281–321

Amon RMW, Benner R (1996) Bacterial utilization of different size classes of dissolved organic matter. Limnol Oceanogr 41:41–51

Anderson LA (1995) On the hydrogen and oxygen content of marine phytoplankton. Deep-Sea Res Part I 42:1675–1680

Barber RT, Smith RL (1981) Coastal upwelling ecosystems. In: Longhurst AR (ed) Analysis of marine systems. Academic Press, San Diego, CA, p 31–68

Benner R (2002) Chemical composition and reactivity. In: Hansell DA, Carlson CA (eds) Biogeochemistry of marine dissolved organic matter. Academic Press, San Diego, CA, p 59–90

Benner R, Pakulski JD, McCarthy M, Hedges JI, Hatcher PG (1992) Bulk chemical characteristics of dissolved organic matter in the ocean. Science 255:1561–1564

Bhosle NB, Bhaskar PV, Ramachandran S (1998) Abundance of dissolved polysaccharides in the oxygen minimum layer of the Northern Indian Ocean. Mar Chem 63:171–182

Børsheim KY, Myklestad SM, Sneli, JA (1999) Monthly profiles of DOC, mono- and polysaccharides at two locations in the Trondheimsfjord (Norway) during two years. Mar Chem 63:255–272

Burney CM, Sieburth JM (1977) Dissolved carbohydrates in seawater: II. A spectrophotometric procedure for total carbohydrate analysis and polysaccharide estimation. Mar Chem 5:15–28

Carlson CA, Ducklow HW, Michaels AF (1994) Annual flux of dissolved organic carbon from the euphotic zone in the northwestern Sargasso Sea. Nature 371:405–408

Castro CG, Álvarez-Salgado XA, Figueiras FG, Pérez FF, Fraga F (1997) Transient hydrographic and chemical conditions affecting microplankton populations in the coastal transition zone of the Iberian upwelling system (NW Spain) in September 1986. J Mar Res 55:321–352

Chavez FP, Toggweiler JR (1995) Physical estimates of global new production: the upwelling contribution. In: Summerhayes CP, Emeis KC, Angel MV, Smith RL, Zeitzschel B (eds) Upwelling in the ocean. Modern processes and ancient records. Wiley and sons, New York, p 13–32

Chen RF, Fry B, Hopkinson CS, Repeta DJ, Peltzer ET (1996) Dissolved organic carbon on Georges Bank. Cont Shelf Res 19:409–420

Clark LL, Ingall ED, Benner R (1998) Marine phosphorus is selectively remineralized. Nature 393:426

Doval MD, Álvarez-Salgado XA, Pérez FF (1997) Dissolved organic matter in a temperate embayment affected by coastal upwelling. Mar Ecol Prog Ser 157:21–37

Fraga F (1967) Hidrografía de la Ría de Vigo 1962, con especial referencia a los compuestos de nitrógeno. Invest Pesq (Spain) 31:145–259

Fraga F (2001) Phytoplanktonic biomass synthesis: application to deviations from Redfield stoichiometry. Sci Mar 65: 153–169

Fraga F, Vives F (1961) La descomposición de la material orgánica nitrogenada en el mar. Invest Pesq (Spain) 19: 65–79

Gilcoto M, Álvarez-Salgado XA, Pérez FF (2001) Computing optimum estuarine residual fluxes with (OERFIM) a multiparameter inverse method: application to the Ría de Vigo (NW Spain). J Geophys Res 106:31303–31318

Haynes R, Barton ED (1990) A poleward flow along the Atlantic coast of the Iberian Peninsula. J Geophys Res 95: 11425–11441

Hedges JI (1992) Global biogeochemical cycles: progress and problems. Mar Chem 39:67–93

Hedges JI (2002) Why dissolved organics matter. In: Hansell DA, Carlson CA (eds) Biogeochemistry of marine dissolved organic matter. Academic Press, San Diego, CA, p 1–33

Hedges JI, Baldock JA, Gélinas Y, Lee C, Peterson ML, Wakeham SG (2002) The biochemical and elemental compositions of marine plankton: a NMR perspective. Mar Chem 78:47–63

Hung CC, Tang D, Warnken KW, Santschi PH (2001) Distribution of carbohydrates, including uronic acids, in estuarine waters of Galveston Bay. Mar Chem 73:305–318

Hung CC, Guo L, Santschi PH, Alvarado-Quiroz N, Haye JM (2003) Distributions of carbohydrate species in the Gulf of Mexico. Mar Chem 81:119–135

Kirchman DL, Ducklow HW, McCarthy JJ, Garside C (1994) Biomass and nitrogen uptake by heterotrophic bacteria during the spring phytoplankton bloom in the North Atlantic Ocean. Deep-Sea Res 141:879–895

McCarthy M, Pratum T, Hedges J, Benner R (1997) Chemical composition of dissolved organic nitrogen in the ocean. Nature 390:150–154

McCave IN, Hall IR (2002) Turbidity of waters over the Northwest Iberian continental margin. Prog Oceanogr 52: 299–313

Myklestad SM, Skanoy E, Hestmann S (1997) A sensitive and rapid method for analysis of dissolved mono- and polysaccharides in seawater. Mar Chem 56:279–286

Norrman B, Zweifel UL, Hopkinson CS Jr., Fry B (1995) Production and utilization of dissolved organic carbon during an experimental diatom bloom. Limnol Oceanogr 40: 898–907

Ogawa H, Tanoue E (2003) Dissolved organic matter in oceanic waters. J Oceanogr 59:129–147

Pakulski JD, Benner R (1994) Abundance and distribution of carbohydrates in the ocean. Limnol Oceanogr 39:930–940

Pettine M, Patrolecco L, Manganelli M, Capri S, Farrace MG (1999). Seasonal variations of dissolved organic matter in the northern Adriatic Sea. Mar Chem 64:153–169

Ríos AF, Nombela MA, Pérez FF, Rosón G, Fraga F (1992) Calculation of runoff to an estuary. Ría de Vigo. Sci Mar 56: 29–33

Ríos AF, Fraga F, Pérez FF, Figueiras FG (1998) Chemical composition of phytoplankton and Particulate Organic Matter in the Ría de Vigo. Sci Mar 62:257–271

Rosón G, Álvarez-Salgado XA, Pérez FF (1997) A non stationary box model to determine residual fluxes in a partially mixed estuary, based on both thermohaline properties. Application to the Ría de Arousa (NW Spain). Est Coast Shelf Sci 44:249–262

Senior W, Chevolot L (1991) Studies of dissolved carbohydrates (or carbohydrate-like substances) in an estuarine environment. Mar Chem 32:19–35

Sherwood CR, Butman B, Cacchione DA, Drake DE, Gross TF, Sternberg RW, Wiberg PL, Williams AJ (1994) Sediment-transport events on the northern California continental shelf during the 1990–1991 STRESS experiment. Cont

Shelf Res 14:1063–1099
Siegenthaler U, Sarmiento JL (1993) Atmospheric carbon dioxide and the ocean. Nature, 365:119–125
Sokal FF, Rohlf FJ (1995) Biometry. Freeman, New York
UNESCO (1985) The international system of units (SI) in oceanography. UNESCO Tech Pap Mar Sci 45
Walsh JJ (1991) Importance of continental margins in the marine biochemical cycling of carbon and nitrogen. Nature 359:53–55
Williams PJleB (1995) Evidence for the seasonal accumulation of carbon-rich dissolved organic material, its scale in comparison with changes in particular material and the consequential effect on net C/N assimilation ratios. Mar Chem 51:17–29
Williams PJleB, Gray RW (1970) Heterotrophic utilization of dissolved organic compounds in the sea. 2. Observations on the response of heterotrophic marine populations to abrupt increases in amino acid concentration. J Mar Biol Assoc UK 50:871–881
Witter AE, Luther GW III (2002) Spectrophotometric measurement of seawater carbohydrate concentrations in neritic and oceanic waters from the U. S. Middle Atlantic Bight and the Delaware estuary. Mar Chem 77:143–156
Wollast R (1998) Evaluation and comparison of the global carbon cycle in the coastal zone and in the open ocean. In: Brink KH, Robinson AR (eds) The sea, Vol 10. John Wiley and sons, New York, p 213–252
Wooster WS, Bakun A, McClain DR (1976) The seasonal upwelling cycle along the eastern boundary of the North Atlantic. J Mar Res 34:131–141
Zimmerman RC, Kremer JN, Dugdale RC (1987) Acceleration of nutrient uptake by phytoplankton in a coastal upwelling ecosystem: a modelling analysis. Limnol Oceanogr 40:299–305

Editorial responsibility: Otto Kinne (Editor), Oldendorf/Luhe, Germany

Submitted: April 8, 2004; Accepted: July 20, 2004
Proofs received from author(s): November 11, 2004